PROCEEDINGS of the
23rd International Congress on Acoustics
9 to 13 September 2019 in Aachen, Germany

A locally implicit time-domain FEM for room acoustics simulation including permeable membrane absorbers

Takumi Yoshida[(1)], Takeshi Okuzono[(2)], Kimihiro Sakagami[(3)]

[(1)]HAZAMA ANDO CORPORATION, Japan, yoshida.takumi@ad-hzm.co.jp
[(2)]Kobe University, Japan, okuzono@port.kobe-u.ac.jp
[(3)]Kobe University, Japan, saka@kobe-u.ac.jp

Abstract

First-order ordinary differential equations (ODEs) based time-domain FEM (TD-FEM) is an attractive time-domain solver for room acoustics simulation. For an idealized case the TD-FEM has fourth-order accuracy in both space and time with explicit algorithm. This paper presents a sound absorber modeling in the first-order ODEs based TD-FEM, addressing permeable membrane (PM) absorbers, which have been used to create comfortable acoustic environments in buildings such as conference rooms, stadiums and swimming pools. However, simple implementation of numerical PM absorber model to the TD-FEM engenders fully implicit algorithm. To overcome the difficulty, an iterative solver for sparse linear systems is locally applied to the TD-FEM. As a consequence, locally implicit first-order ODEs based TD-FEM for sound field analyses including PM absorbers is presented. Numerical experiments including acoustics simulation in a real sized room showed that the presented locally implicit TD-FEM performs better than the fully implicit implementation without the reduction of accuracy.

Keywords: Room acoustics simulation, Time-domain FEM, Permeable membrane absorber, Iterative method

1 INTRODUCTION

Wave-based acoustics simulation methods in the time domain, which discretize the wave equation numerically in both space and time, are one of tools for room acoustics design. Recently developed efficient time domain wave-based methods can simulate sound propagation in rooms with simple boundary conditions at frequencies up to several kilohertz. Among various time domain methods, the time domain finite element method (TD-FEM) has an inherent strength in dealing with complex-shaped room model [1, 2, 3]. In standard formulation, TD-FEM shows an implicit algorithm. Therefore, the authors have been presented an efficient implicit time marching scheme using dispersion-reduced low-order finite elements, stability relaxed time integration method and iterative solvers for large-scale room acoustics simulation and it has fourth-order accuracy in both space and time for an idealized condition [2, 3]. Also, as an alternative formulation, the authors are exploring an accurate explicit formulation, which is based on first-order ordinary differential equations (ODEs) [4, 5, 6]. The present paper deals with the latter first-order ODEs based TD-FEM.

Time domain sound absorbers modeling, which can consider both frequency and incident angle dependence of absorption characteristics, is one of the primary concerns to increase the accuracy and applicability of time domain methods for room acoustics simulation. Various absorbers such as porous absorbers and Helmholtz resonator have been used to control acoustics inside buildings. Among them permeable membrane (PM) absorbers, which are air-permeable thin fabrics, are an attractive absorber with its superior material properties, and have been applied successfully to various architectural spaces like conference rooms, and swimming pools. Acoustic curtains, suspended acoustic ceilings and space sound absorbers exemplify PM absorbers. The present paper specifically addresses how to incorporate PM absorbers into the first-order ODEs based TD-FEM efficiently.

In an earlier work [6], we have been presented that the direct implementation of numerical PM model into the first-order ODEs based TD-FEM engenders a fully implicit time marching scheme because the matrix expressing the contribution of permeable membrane cannot be diagonalized. Although the resulting linear system of equa-

tions can be solved efficiently by using an iterative solver, the scheme loses the advantage of explicit algorithm. Therefore, the present paper proposes a locally-implicit time marching scheme to alleviate the difficulty. The locally-implicit scheme is realized by local application of linear equation solver to linear system of equations, which have small unknown, associated with permeable membranes. In doing so, the most part of time marching scheme can be explicit. In the remainder of present paper, the formulation of first-order ODEs based TD-FEM for room acoustics simulation including PM sound absorbers is presented firstly. Secondly, the locally-implicit time marching scheme is proposed. Then, the validity and performance of the present scheme are examined through two numerical examples including acoustics simulation inside practical sized meeting room with PM ceiling absorbers.

2 THEORY

2.1 First-order ODEs based TD-FEM

We consider a closed sound field Ω_f surrounded with a boundary Γ, which is governed by the nonhomogeneous wave equation expressed by

$$\frac{\partial^2 p}{\partial t^2} - c_0^2 \nabla^2 p = \rho_0 c_0^2 \frac{\partial q}{\partial t}, \tag{1}$$

where p, c_0, ρ_0 and q represent, respectively, the sound pressure, the speed of sound, the air density and the added fluid mass per unit volume. ∇ represents the gradient of a variable. The weak from of nonhomogeneous wave equation is expressed by

$$\int_{\Omega_\mathrm{f}} \phi_\mathrm{f} \frac{\partial^2 p}{\partial t^2} dV + c_0^2 \int_{\Omega_\mathrm{f}} \nabla \phi_\mathrm{f} \nabla p \; dV = c_0^2 \int_{\Gamma_\mathrm{f}} \phi_\mathrm{f} \frac{\partial p}{\partial n} dA + \rho_0 c_0^2 \int_{\Omega_\mathrm{f}} \phi_\mathrm{f} \frac{\partial q}{\partial t} dV. \tag{2}$$

Here, ϕ_f denotes the arbitrary weight function. Introducing Galerkin finite element method to the sound pressure and weight function in the weak form, with three boundary conditions, i.e., a rigid boundary, a vibrating boundary and an impedance boundary, gives the following semi-discrete second-order ODE as

$$\mathbf{M}\ddot{\mathbf{p}} + c_0^2 \mathbf{K}\mathbf{p} + c_0 \mathbf{C}\dot{\mathbf{p}} = \mathbf{f}, \tag{3}$$

where $\mathbf{M}$, $\mathbf{K}$ and $\mathbf{C}$ respectively denote the global mass matrix, the global stiffness matrix, and the global dissipation matrix. $\mathbf{p}$ and $\mathbf{f}$ respectively denote the sound pressure vector, the external force vector. The symbols $\cdot$ and $\cdot\cdot$ signify first- and second-order time derivatives. For the explicit calculation of Eq. (3), a diagonal mass matrix $\mathbf{D}$ lumped from $\mathbf{M}$ and a vector $\mathbf{v} = \dot{\mathbf{p}}$ are introduced. Consequently, Eq. (3) is transformed into

$$\mathbf{D}\dot{\mathbf{p}} = \mathbf{M}\mathbf{v}, \tag{4}$$

$$\mathbf{D}\dot{\mathbf{v}} = \mathbf{f} - c_0^2 \mathbf{K}\mathbf{p} - c_0 \mathbf{C}\dot{\mathbf{p}}. \tag{5}$$

In temporal direction, $\dot{\mathbf{p}}$ in Eq. (4) and $\dot{\mathbf{v}}$ in Eq. (5) are respectively discretized using first-order accurate forward difference and backward difference. The resulting time marching scheme is expressed as follow [5].

$$\mathbf{p}^n = \mathbf{p}^{n-1} + \Delta t \mathbf{D}^{-1} \mathbf{M} \mathbf{v}^{n-1}, \tag{6}$$

$$(\mathbf{D} + \Delta t c_0 \mathbf{C}) \mathbf{v}^n = \mathbf{D}\mathbf{v}^{n-1} + \Delta t (\mathbf{f}^n - c_0^2 \mathbf{K}\mathbf{p}^n). \tag{7}$$

Here, n and Δt respectively represent the time step and the time interval. Note that Eq. (7) is solvable explicitly with a lumped dissipation matrix $\mathbf{C}$. Furthermore, the first-order ODEs based TD-FEM achieves fourth-order accuracy in both space and time using MIR for an idealized condition [4, 5].

2.2 Time-domain FE modeling of PM absorber

In this study, a limp membrane with the surface density M and the flow resistance R is assumed. Figure 1 shows FE model of PM, where $\Omega_{\mathrm{e,f}}$, $\Gamma_{\mathrm{e,M}}$, $\Gamma_{\mathrm{e,Ma}}$ and $\Gamma_{\mathrm{e,Mb}}$ respectively represent the air element, the PM

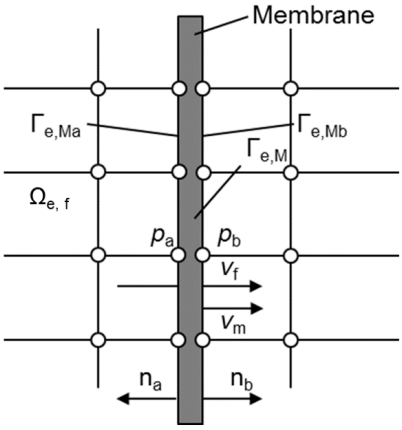

Figure 1. FE model of PM.

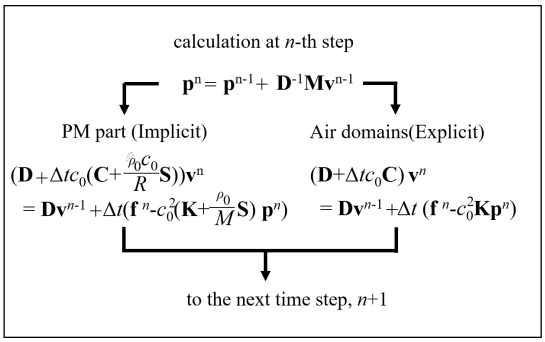

Figure 2. The algorithm of locally-implicit time marching scheme for acoustics simulation including PM sound absorbers.

element and the boundary surfaces of both sides of PM. The sound pressure of two sides of PM is represented by p_{a} and p_{b}. v_{f} and v_{m} are the particle velocity near and inside PM, and the vibration velocity of PM. The equation of motion for limp PM is given by

$$M\dot{v}_{\mathrm{m}} = p_{\mathrm{a}} - p_{\mathrm{b}}, \tag{8}$$

The air permeability of PM is expressed by the flow resistance, which is defined as

$$R = \frac{p_{\mathrm{a}} - p_{\mathrm{b}}}{v_{\mathrm{f}} - v_{\mathrm{m}}}. \tag{9}$$

Using Eqs (8), (9), a PM can be modeled by imposing the following vibration boundary conditions on both boundary surfaces $\Gamma_{\mathrm{e,Ma}}$ and $\Gamma_{\mathrm{e,Mb}}$.

$$\frac{\partial p}{\partial n} = \begin{cases} -\rho_0 \dot{v}_{\mathrm{f}} & \text{on } \Gamma_{\mathrm{e,Ma}} \\ \rho_0 \dot{v}_{\mathrm{f}} & \text{on } \Gamma_{\mathrm{e,Mb}}. \end{cases} \tag{10}$$

Table 1. Three types of PMs (PM A, PM B and PM C) with the different surface density M and the flow resistance R.

Type	M, kg/m^2	R, Pa s/m^3
A	0.065	196
B	0.120	462
C	0.495	1087

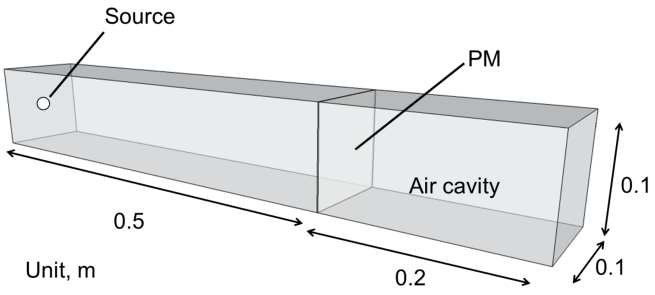

Figure 3. An analyzed impedance tube model with a single-leaf PM absorber.

By considering the above vibration boundary condition, the second equation in the time marching scheme of first-order ODEs based TD-FEM (Eq. (7)) is rewritten as

$$[\mathbf{D}+\Delta t c_0(\mathbf{C}+\frac{\rho_0 c_0}{R}\mathbf{S})]\mathbf{v}^n = \mathbf{D}\mathbf{v}^{n-1}+\Delta t[\mathbf{f}^n - c_0^2(\mathbf{K}+\frac{\rho_0}{M}\mathbf{S})\mathbf{p}^n]. \tag{11}$$

Here, the global matrix $\mathbf{S}$ denotes the contribution of PM. Because $\mathbf{S}$ cannot be lumped, it engenders non-diagonal components to the coefficient matrix. Therefore, Eq. (11) becomes implicit and must be solved at each time step using linear equation solvers. The CG solver with diagonal scaling preconditioning is used for the solution. The convergence tolerance is set to 10^{-6}.

3 LOCALLY-IMPLICIT SCHEME

When addressing PM sound absorbers, the first-order ODEs based TD-FEM becomes an implicit method as presented in 2.2. However, the coefficient matrix of Eq. (11) has non-diagonal components only in the rows corresponding to nodes on surfaces of PM. Therefore, the linear equations of Eq. (11) can be solved by local application of iterative methods to PM part. Then, air domains are calculated using Eq. (7), explicitly. Figure 2 shows the algorithm of locally-implicit time marching scheme.

Regarding the reduction of computational costs by locally-implicit scheme, a total number of sparse matrix-vector products (N_{SMVP}), which is the main operation of TD-FEM, for fully implicit scheme is defined by

$$N_{\mathrm{SMVP,full}} = N_{\mathrm{step}} \times 2 + N_{\mathrm{iter}}, \tag{12}$$

where N_{step} and N_{iter} respectively represent the total number of time steps and the total number of iterations. Here, the fully implicit scheme means that Eq. (11) is used in both PM part and air domains. The first term of Eq. (12) means N_{SMVP} for $\mathbf{M}\mathbf{v}$ in Eq. (6) and $(\mathbf{K}+\frac{\rho_0}{M}\mathbf{S})\mathbf{p}$ in Eq. (11). The second term expresses N_{SMVP} for

Table 2. Calculation conditions of two meshes

Mesh	h, m	Δt, s	r_{DOF}
1	0.005	1/131000	0.014
2	0.05	1/10400	0.143

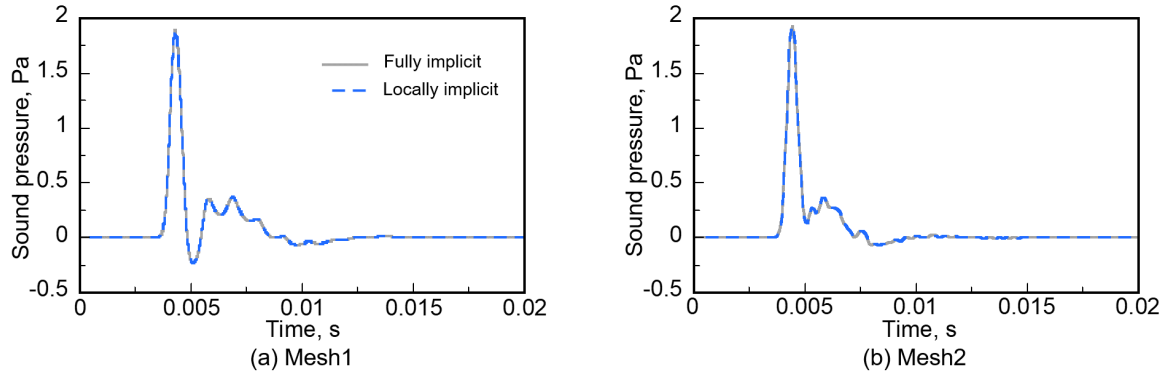

Figure 4. Comparisons of waveforms for PM C between the fully implicit scheme and locally-implicit scheme in the case with (a) Mesh 1 and (b) Mesh 2

iterative operations in CG method. On the other hand, N_{SMVP} of the locally-implicit scheme is expressed as

$$N_{\mathrm{SMVP,local}} = N_{\mathrm{step}} \times 2 + r_{\mathrm{DOF}} \times N_{\mathrm{iter}}, \tag{13}$$

with

$$r_{\mathrm{DOF}} = \frac{N_{\mathrm{PM}}}{N_{\mathrm{All}}}. \tag{14}$$

Here, N_{PM} and N_{All} denote a number of nodes on the PM and all nodes, respectively. In Eq. (13), N_{SMVP} for **Mv** of Eq. (6) and **Kp** of Eq. (7) are represented as the first term. The second term means that N_{SMVP} for iterative operations in CG method can be reduced to r_{DOF} times that of the fully implicit scheme. The locally-implicit scheme can reduce N_{SMVP} significantly, because N_{PM} is generally much lower than N_{All}.

4 NUMERICAL EXPERIMENTS

The validity and numerical efficiency of the locally-implicit scheme were investigated using an impedance tube model and a real sized meeting room model [6]. As listed in Table 1, three types of PMs, each with different M and R, were used in the two models. The most classical single-leaf PM absorber consisting of PM and rigid-backed air cavity was considered. To verify the proposed scheme, waveforms calculated using the fully implicit scheme and locally-implicit scheme were compared. Moreover, the efficiency was evaluated using the following measure r_{NSMVP}.

$$r_{\mathrm{NSMVP}} = \frac{N_{\mathrm{SMVP,local}}}{N_{\mathrm{SMVP,full}}}. \tag{15}$$

Table 3. r_{NSMVP} for PM A∼C in the cases using Mesh 1 and Mesh 2.

	PM A	PM B	PM C
Mesh 1	41.0	42.7	41.6
Mesh 2	35.8	37.5	41.1

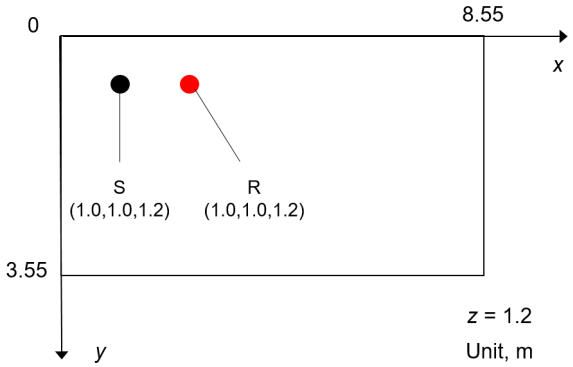

Figure 5. A plane at 1.2 m height of the meeting room on which a source point S and receiving point R are located.

4.1 Impedance tube model

Figure 3 shows an impedance tube model with a single-leaf PM absorber of 0.2 m air cavity depth. A source was located on the tube inlet. A receiving point was placed at 0.05 m in front of PM. A modulated Gaussian pulse with the upper limit frequency of 1500 Hz was used as a sound source. As for boundary conditions, the tube inlet is absorbing boundary with the characteristic impedance of air and other boundaries are treated as rigid walls. Waveforms up to 0.1 s were calculated using two FE meshes (Mesh 1 and Mesh 2) with different spatial resolution. Table 2 lists the mesh size h, Δt and r_{DOF} for Mesh 1 and Mesh 2.

Figure 4 shows comparisons of waveforms for PM C between fully implicit and locally-implicit schemes in the cases using Mesh 1 and Mesh 2. In both meshes, the waveforms between both schemes agree well each other. Similar results were obtained in other cases. Table 3 shows r_{NSMVP}s for the cases using Mesh 1 and Mesh 2. Using the locally-implicit scheme reduces N_{SMVP} to 35.8 $\sim$ 42.7% of those in the fully implicit scheme.

4.2 Meeting room model

Rectangular meeting room (8.55 m in length, 3.55 m in width, and 3.0 m height) with PM ceiling absorber was analyzed as a demonstration of practical case. A single-leaf PM absorber with air cavity of 0.1 m was installed on the ceiling. A point source S and a receiver R were located on a plane of 1.2 m height, as shown in Fig. 5. 1/3 octave band-limited impulse responses were calculated at 500 Hz and 1 kHz with a source signal of impulse response of IIR filter. Regarding boundary conditions, a real-valued equivalent impedance $z_{\mathrm{e}} = 126.3$ was given to the walls and the floor. The impedance value corresponds to a statistical absorption coefficient 0.059. The FE mesh used here is created to satisfy a spatial resolution of 6.1 elements per wavelength at the upper-limit frequency of 1 kHz 1/3 octave band. In the analysis, r_{DOF} equals to 0.031, which can expect the significant benefit of locally-implicit scheme. Impulse responses were calculated up to 2.0 s with $\Delta t = 1/10400$ s.

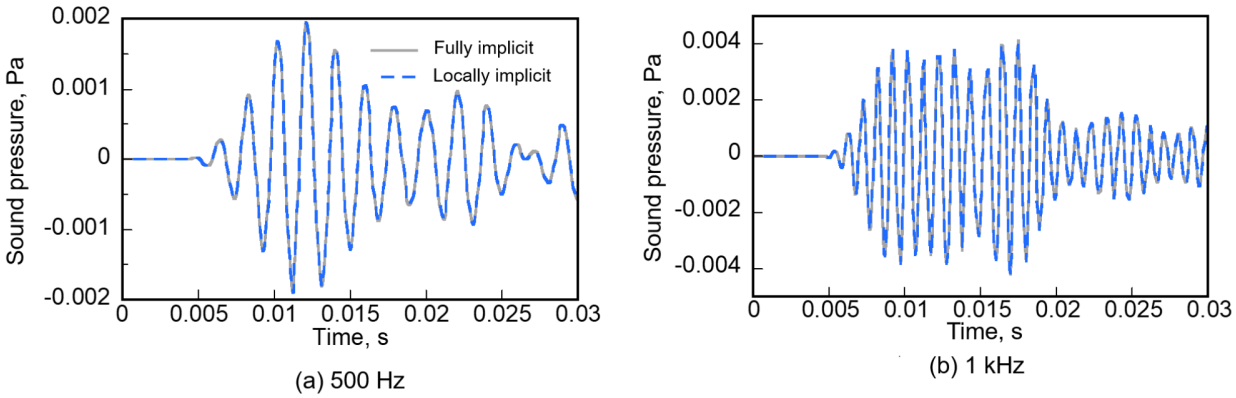

Figure 6. Comparisons of waveforms between the fully implicit scheme and locally implicit scheme at (a) 500 Hz and (b) 1 kHz in the case using PM C.

Table 4. r_{NSMVP} for PM A∼C at 500 Hz and 1000 Hz.

	PM A	PM B	PM C
500 Hz	21.5	25.6	32.5
1000 Hz	21.0	24.9	31.2

Figure 6 shows comparisons of waveforms in the case using PM C between both schemes up to 0.03 s, including reflections from the ceiling absorber. The waveforms calculated using the locally-implicit scheme agree well with those using the fully implicit scheme. As shown in Table 4, the locally-implicit scheme is 3.08 $\sim$ 4.76 times faster than the fully implicit scheme, which indicates clearly the effectiveness of locally-implicit scheme.

CONCLUSION

The presented paper proposed the locally-implicit TD-FEM based on first-order ODEs for room acoustics simulation including PM absorbers. Numerical experiments demonstrated the efficiency of present scheme over fully implicit scheme without reducing accuracy.

REFERENCES

[1] Okuzono T., Otsuru T., Tomiku R. and Okamoto N., Fundamental accuracy of time domain finite element method for sound field analysis of room, *Applied Acoustics*, **71**(10), 940–946, (2010).

[2] Okuzono T., Otsuru T., Tomiku R. and Okamoto N., Application of modified integration rule to time-domain finite-element acoustics simulation of rooms , *The Journal of the Acoustical Society of America*, **132**(2), 804–813, (2012).

[3] Okuzono T., Shimizu N., Sakagami K., Predicting absorption characteristics of single-leaf permeable membrane absorbers using finite element method in a time domain, *Applied Acoustics*, **151**, 172–182, (2019).

[4] Okuzono T., Yoshida T., Sakagami K. and Otsuru T. An explicit time-domain finite element method for

room acoustics simulations: Comparison of the performance with implicit methods, *Applied Acoustics*, **104**, 76–84, (2016).

[5] Yoshida T., Okuzono T., Sakagami K., Numerically stable explicit time-domain finite element method for room acoustics simulation using an equivalent impedance model, *Noise Control Engineering Journal*, 66(3), 176–189 (1 May 2018).

[6] Yoshida T., Okuzono T., Sakagami K., A three-dimensional time-domain finite element method based on first-order ordinary differential equations for treating permeable membrane absorbers, *Proceedings of the* 25^{th} *International Congress on Sound and Vibration*, Hiroshima, 8–12 July, (2018).